

Finite Element Formulations for Fast Computation of Large and Moderately Large Deformations

D. Marinković and M. Zehn
Structural Mechanics Department
Technical University Berlin, Germany

Abstract

The paper presents finite element formulations aimed at fast computation of large and moderately large flexible body deformations in the fields of virtual reality technology and multibody dynamics. In many areas of application, virtual reality requires real-time or nearly real-time simulation of deformable objects' behaviour, quite often with deformations involving large local rotations. The well-known simplified approach based on mass-spring systems is shortly discussed with advantages and disadvantages pointed out. This is followed by a co-rotational 3D-FEM approach based on rigid-body rotations performed on element level. The approach accounts for large local rigid-body rotations and yields satisfying accuracy combined with high numerical efficiency. Since force feedback is very important in certain virtual reality applications, special attention is given to the issue. Furthermore, novel formulations for consideration of geometrical nonlinearities in the modal space are presented. For bodies which do not undergo large configuration changes throughout the deformation, an approach based on inclusion of the geometric stiffness matrix is proposed. The second approach is aimed at nonlinearities, which are a consequence of moderately large rotations of some parts of the flexible body. Examples for all proposed approaches are provided, demonstrating their characteristics.

Keywords: geometrically nonlinear analysis, real-time simulation, virtual reality, co-rotational FEM formulation, modal space, multi-body dynamics.

1 Introduction

Physically based real-time simulation is inherently a multidisciplinary field that combines mechanics, numerical calculation and computer graphics – to name only a few. Computer simulated environments comprising dynamically deforming objects, which can be interacted with, represent the background of the approach. Although

the quality of the animation and rendering determines the very first impression of the achieved results, it is actually the displayed physical behaviour of the objects that eventually determines the simulation quality, i.e. the degree of realism exhibited by the simulated environment. This imposes the need to work with models that determine the objects' behaviour based on physical laws. A noticeable contribution to the field has been made by developers in the field of computer graphics (e.g. [1]), who needed to go beyond their field of expertise and grasp the basics of material mechanical behaviour.

In the past decades, a number of methods has been developed with the aim of predicting physical behaviour of deformable objects with very high level of accuracy. The finite element method (FEM), as dominant one in the field, has deservedly gained the reputation of the 'state-of-the-art method'. The off-line FEM calculations pose accuracy as the primary simulation objective, as it is aimed at authentic representation of the real world. Numerical efficiency, i.e. the CPU time needed for the calculation, always plays an important role, of course, but not as crucial as it does in the case of real-time computations. In real-time simulations, the computational efficiency plays the primary role and a trade-off between this requirement and the reached accuracy of computation has to be made. This means that different approximations are acceptable, whereby the limits of reducing accuracy are defined by the requirements of the actual field of application. Mainly for historical reasons, the paper gives at first a short consideration of the approach based on mass-spring systems, which was in the researchers' focus in the last decades [1, 2, 3]. The attention is then turned to a 3D FEM co-rotational approach that accounts for large local rotations on the element level, thus offering a good compromise between the required numerical effort and achieved accuracy in the field of geometrically nonlinear analysis.

In the second part, the focus of the paper is shifted to the field of multibody dynamics for engineering purposes. Programs for simulating dynamics of multibody systems (MBS) are originally developed for rigid bodies. On the other hand, many physical systems require consideration of flexible bodies in MBS for an adequate simulation of their behaviour. In order to retain numerical efficiency this is done in modal space, which intrinsically allows consideration of only elastic deformations within the local coordinate system of the flexible body. However, certain assumptions would allow extensions of the approach aiming at approximations for geometrically nonlinear behaviour. The first extension is applicable to bodies which do not undergo large configuration changes during the deformation, so that the nonlinear effects are mainly a consequence of stress stiffening. The second extension is developed for deformations, in which some parts of the flexible body perform moderately large rotations with respect to the rest of the body.

2 FEM formulations for real-time simulations

Firstly, formulations for full FEM models, i.e. without model reduction, aimed at real-time simulation of large deformations are presented. To make it more precise, the term 'large deformation' refers here to geometrically nonlinear deformations, primarily to those characterized by large local rigid-body rotations. In order to

achieve good numerical efficiency, a kind of simplified geometrically nonlinear formulation is sought, but which provides results with acceptable deviation from those of the ‘full’ geometrically nonlinear formulation. Minimum of the requirement is simulation yielding physically plausible behaviour, since in many virtual reality applications this is the only requirement.

2.1 Mass-spring systems

Of all deformable models, this one is arguably the simplest and most intuitive one. This is the main reason for the large interest in it during the previous decade. A model based on mass-spring systems consists of a collection of point masses connected by a network of massless springs. The springs are commonly modelled as linearly elastic, although it would not demand a too great effort to extend such a model to account for nonlinear behaviour of the springs and furthermore to model plasticity.

Adopting the model with linearly elastic springs, the necessary parameters that define properties of a spring are the spring stiffness coefficient, k , damping coefficient, d , and initial (unloaded) length of the spring, l_0 . The topology defines how the masses are connected to each other. Once the parameters and topology are given, it is a straightforward task to determine the internal elastic and damping forces, i.e. the forces due to deformation of the springs connected to mass m_j and due to relative velocity of the mass m_j with respect to other masses connected with it by springs. Regardless of the current configuration of the system, the intensity and orientation of the forces is easily determined, since they always act along the springs, i.e. along the straight lines between interconnected masses and, thus, the geometrical nonlinearities are easily accounted for. Let us assume that the point mass m_j is connected to n_{mj} point masses listed as $m_j(i)$, $i = 1, \dots, n_{mj}$, by the same number of springs, listed as $k_{mj}(i)$ and $d_{mj}(i)$, $i = 1, \dots, n_{mj}$. Then, the internal elastic force and internal damping force acting on mass m_j are respectively given by the following expressions:

$$\vec{F}_{e_j} = \sum_{i=1}^{n_{mj}} k_{mj}(i) (\vec{v}_{m_j(i)} - \vec{v}_j) \left(I - \frac{l_{0i}}{|\vec{v}_{m_j(i)} - \vec{v}_j|} \right) \quad (1)$$

$$\vec{F}_{d_j} = \sum_{i=1}^{n_{mj}} d_{mj}(i) \frac{(\vec{v}_{m_j(i)} - \vec{v}_j)}{|\vec{v}_{m_j(i)} - \vec{v}_j|^2} \left((\vec{v}_{m_j(i)} - \vec{v}_j) \cdot (\dot{\vec{v}}_{m_j(i)} - \dot{\vec{v}}_j) \right) \quad (2)$$

where index i runs over all n_{mj} point masses connected with the point mass m_j and \vec{v}_i is, generally, the vector defining the position of mass m_i in the global coordinate system (x, y, z).

The authors of the paper have used this approach in combination with a relatively simple explicit time integration procedure, thus avoiding the need to build complete structural (mass and stiffness) matrices as well as to perform matrix inversions. Hence, the equations are decoupled but the time-step is severely limited by the

stability requirements of the method and depends on the highest eigenfrequency of the system. During simulation, the structure may undergo significant configuration changes, which affects its eigenfrequencies, and one has to be conservative in the choice of the critical time-step. Another possibility would be a continuous (online) update of the critical time-step. Which option is more efficient depends on how significant changes of the highest eigenfrequency may occur during simulation.

The significant advantage of the mass-spring system is that it handles large deformations with ease, it is computationally very efficient and easy to implement. On the other hand, mass-spring systems have a significant accuracy problem and the results are quite dependent on mesh resolution and topology. The ambiguity of mass and structural stiffness distribution is another serious drawback. Preserving the volume of the initial configuration and the configuration itself upon removing external loads is also an issue with this approach. The recent survey by Nealen, et al., [3] gives a good overview of possible problems and solutions offered by different authors for the mass-spring systems.

2.1.1 Examples of application

The examples are simple and serve only to obtain a rather general impression on the approach and achievable results. Figure 1 shows the application of the mass-spring system to model a quasi 2D-structure – a cloth. Large deformations during an interactive simulation are shown in the figure. Figure 2 shows the same approach used to model a 3D-structure. The depicted cube consists of cell-cubes, whereby the masses within each cell-cube are interconnected by springs along edges, face diagonals and room diagonals of the cell-cube. Both figures depict a wire model in order to exemplify the proposed mass distribution and topology of spring connections.

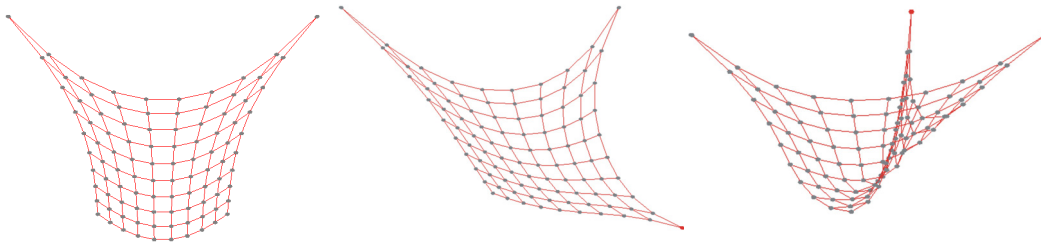


Figure 1: Application of mass-spring system to model a 2D-structure - cloth

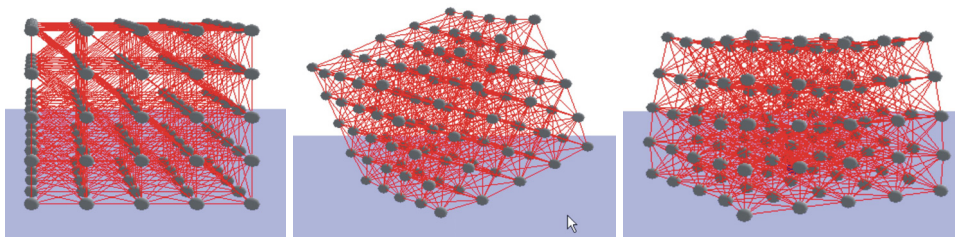


Figure 2: Application of mass-spring system to model a 3D-structure – cube

2.2 Continuum-based FEM approach

The availability of powerful hardware in the last decade resulted in a trend to develop models for real-time simulations that are more sophisticated than mass-spring systems. Continuum-based FEM approach is certainly more expensive, but offers the advantage of better accuracy regarding both, the description of material properties and 3D material behaviour.

Models for real-time simulation are supposed to be stable and computationally as inexpensive as possible. Linear FEM models are suitable regarding both requirements, but cannot adequately represent geometrically nonlinear deformations. It should be emphasized that, as long as deformations remain in the realm of materially linear behaviour, translations are easily handled with linear models, but already moderate rotations suffice to deteriorate the accuracy of the linear FEM results beyond the limit of applicability, even if only visual representation of deformation is of interest. On the other hand, geometrically nonlinear formulations, in their theoretically pure form, offer more than a satisfying degree of accuracy, but are rather expensive for real-time simulations and may also exhibit problems with simulation stability. A relatively simple formulation that is supposed to combine the advantages and avoid the drawbacks of the previous two is offered in this paper.

The basic idea of the formulation is rather simple and originates from the principles of incorporating flexible bodies in Multi-Body-System (MBS) dynamics. In MBS dynamics the overall motion of flexible bodies is given as a superposition of large rigid-body motion and small deformation with respect to a local body-fixed coordinate system (c.s.) that, of course, performs the same rigid-body motion as the body itself. In this manner, the local c.s. excludes large rotation from the body motion, thus allowing to extract the deformable motion up to a great extent. The idea can be extended so that each element of the finite-element assemblage is assigned a local c.s., with respect to which the behaviour of the element remains purely linear. The approach permits handling deformations in which parts of the flexible body perform large rotations with respect to the remaining of the body, as already recognized by Etmuss et al. [4].

This concept allows the calculation of linear stiffness matrices of single elements, \mathbf{K}_e , in a pre-step prior to interactive simulation. In real-time it is necessary to use the information about the last determined and the original configuration in order to extract rigid-body rotation for each single element, described by the rotational matrix \mathbf{R}_e . Once the rotation is known, the last determined configuration of the element is rotated back, i.e. through \mathbf{R}_e^{-1} . The so-obtained configuration is compared with the initial configuration to determine the displacements free of rigid-body rotation. Multiplication of the element stiffness matrix with rotation-free displacements yields internal elastic forces of the element in the original frame of the element. What remains is to rotate the forces to the current element frame, i.e. through \mathbf{R}_e . The described operations are summarized in the following expression:

$$\vec{F}_e = \mathbf{R}_e \mathbf{K}_e (\mathbf{R}_e^{-1} \vec{v}_e - \vec{v}_{0e}) \quad (3)$$

where \vec{v}_{0e} and \vec{v}_e are the initial and current element configurations, respectively. And rearranging Equation (3) one obtains:

$$\vec{F}_e = \mathbf{R}_e \mathbf{K}_e \mathbf{R}_e^{-1} \vec{v}_e - \mathbf{R}_e \mathbf{K}_e \vec{v}_{0e} = \mathbf{K}_e^R \vec{v}_e - \vec{F}_{0e}^R \quad (4)$$

where \mathbf{K}_e^R denotes the rotated element stiffness matrix. Thus, the essence of the concept consists in rotation of each element linear stiffness matrix.

Another important aspect is the time integration scheme and solver. Of course, the approach may be used in combination with an explicit time integration scheme, the basic properties of which are already briefly discussed in the section handling mass-spring systems. However, it should be kept in mind that the formulation aims at virtual reality applications, where human perception plays a major role. Since human eye may register a limited number of pictures per second, high frequency behaviour is often (but not always) of less interest in virtual reality applications. Hence, the authors take advantage of an implicit time integration scheme, which is indeed more expensive regarding the necessary computational effort for a single time-step, but, on the other hand, allows significantly larger time-steps compared to an explicit solver. The implicit time integration scheme keeps the coupled system of equations and, thus, requires forming the complete stiffness matrix of the structure and solving the system. Instead of commonly used direct solvers, the authors use an iterative solution procedure – the preconditioned conjugate gradient method (more details in [5]), which benefits from the system matrix in the sparse form. The method is very convenient for real-time simulations. First of all, the conjugate gradient method involves one matrix-vector product, three vector updates, and two inner products per iteration, which makes it computationally very attractive for nonlinear systems. Furthermore, it provides a very easy way of performing a trade-off between the solution accuracy and computational effort by limiting the number of performed iterations.

2.2.1 Examples – aspect of accuracy

As it has been mentioned above, the presented co-rotational formulation is supposed to combine advantages of the linear and geometrically nonlinear FEM formulations and, as much as possible, try to eliminate their disadvantages. Whereas it is obviously numerically much more efficient than the full geometrically nonlinear formulation, the price to be paid for this advantage is reduced accuracy of the results, since not all of the geometrically nonlinear effects are accounted for, such as change of element configuration with respect to the local c.s. or stress stiffening effects.

A very simple example is given here to provide a hint about this aspect of the proposed formulation. A solid block made of steel ($E=2.1 \times 10^{11}$ Pa, $\nu=0.3$) with dimensions $5 \times 5 \times 1.5$ m is considered. The force of 1.3×10^{10} N acts in the negative z-direction, as depicted in Figure 3a. The geometry is discretized with 863 linear tetrahedral elements. The considered model is rather simple and the authors are aware of the fact that it is not adequate for the purpose of analysis of the considered structure's behaviour. The sole purpose of the model is to compare the results that

different formulations yield with exactly the same FEM model. The force is chosen so that obvious geometrically nonlinear effects are caused (material nonlinearities are neglected, as they are not the subject of interest here). The deformation is calculated by means of linear, ‘full’ geometrically nonlinear and proposed formulation. The linear and the full geometrically nonlinear analysis are done in commercially available FEM software package ABAQUS. Figures 3b and 3c show the (unscaled) deformed configurations of the structure calculated in ABAQUS (taken from ABAQUS postprocessor) and by means of present formulation (graphics programmed by authors in OpenGL), respectively.

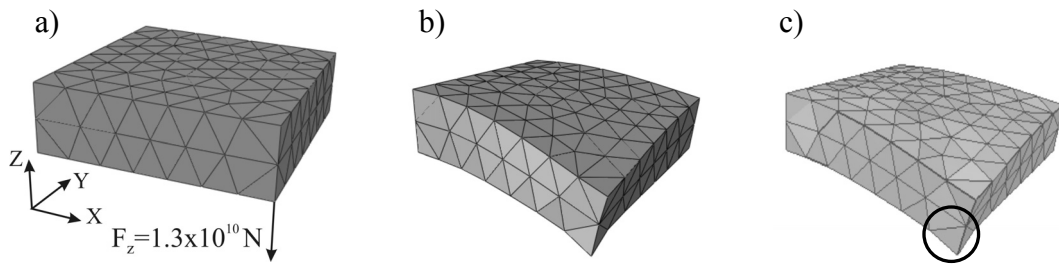


Figure 3: A solid block: a) initial configuration with excitation force; b) nonlinear result by ABAQUS; c) result by present formulation

The point at which the force acts is chosen to compare the results from ABAQUS and the proposed formulation. The calculated displacements of the point in all three global directions are given in Figure 4. It should be emphasized that the linear results from ABAQUS and the linear result with the tetrahedral element used by authors match exactly, so that the differences in nonlinear results seen in Figure 4 are only the consequence of different formulations.

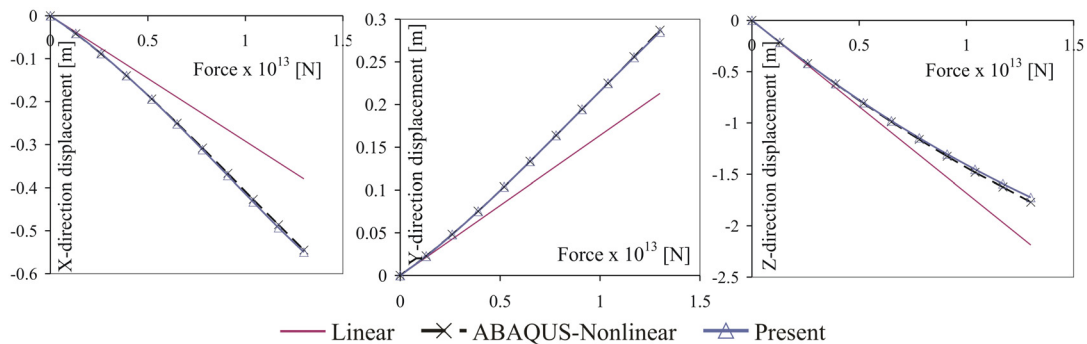


Figure 4: Linear and geometrically nonlinear results for displacements in global x-, y- and z-direction, respectively

One should notice that the considered point, in fact, is not the optimal choice for the comparison purposes. This is due to the fact that it is the node at which the force acts and that this node belongs to only one element (pointed out in Figure 4c). The concentrated force results in singularity and relatively large deformation of the considered element compared to other elements. Thus, the influence of deformation

of one single element on the obtained results is greater than normally expected. As already mentioned, the change of element configuration in the local c.s. is not accounted for by the proposed co-rotational formulation, as opposite to ABAQUS. A sharp eye may even recognize that the considered element exhibits different deformations in Figures 3b and 3c. However, this only means that the point represents a conservative choice for the comparison purpose, which speaks in favour of good agreement of the nonlinear results seen for each of the three global displacements in Figure 4. Though for the sake of brevity it is not given here, the agreement is even better for the remaining nodes.

2.2.2 Examples – aspect of plausibility of deformational behaviour

In many virtual reality applications it is enough to reproduce a plausible deformational behaviour of flexible bodies. The accuracy plays a minor role and is not particularly specified. The linear FE formulation is known for producing artificial enlargement of structures under deformation that involves large rotations. Such behaviour is not plausible to human perception. A simple example given in Figure 5 demonstrates this effect. A simple thin-walled structure (only mid-surface depicted), which has a plain form in original, undeformed configuration is considered. Figure 5a shows a deformed configuration as calculated by linear FEM formulation, while Figure 5b demonstrates the result yielded by the present formulation. A quadratic hexahedral element is used in the example.

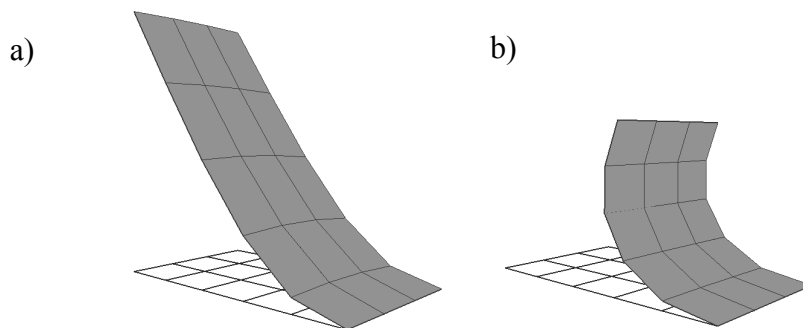


Figure 5: Plausibility of deformational behaviour of a thin-walled structure

The presented concept in combination with hardware of an ‘average pc’ allows models with several thousand elements at interactive frame rate. However, in most cases a volumetric mesh with such a number of elements still cannot offer an appealing representation of surface, when objects of rather complex geometry are modelled. If it is aimed at plausible behaviour only, the idea on how to cope with the problem consists in introducing two meshes – a volumetric FE-mesh, which is used to calculate the deformation and a detailed triangularized surface mesh, which is used to represent the actual, complex geometry of the object. As a pre-step of the interactive simulation the two meshes are coupled to each other. For each vertex of the surface mesh a corresponding finite element is found and the surface vertex is assigned to this element. The criterion to find the corresponding element is based on

the local coordinates of the vertex with respect to the elements. The local coordinates reveal if the vertex is placed inside an element. If that is the case, the vertex is assigned to that element. In some cases the FE-mesh may be chosen so that this criterion does not yield a corresponding element for some of the surface vertices. This is the case when some of the surface vertices are placed outside the FE-mesh. This would be detected by the check performed on local coordinates followed by a search for an element, for which the sum of absolute values of vertex local coordinates takes a minimum value and the vertex is finally assigned to that element.

A model of a dog shown in Figure 6 (courtesy of Matthias Müller, NVidia Switzerland), illustrates the above described approach. The FE-mesh (700 elements, 314 nodes) of the model is given in Figure 6a. Figure 6b depicts 12520 surface vertices, which are connected to form the topology of a triangularized surface – 24835 faces (Figure 6c), which can be covered by a texture to provide a realistic appearance (Figure 6d).

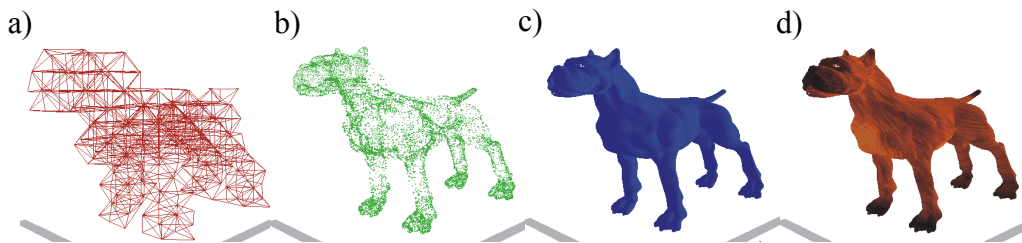



Figure 6: Model of a dog: a) FE-mesh; b) surface vertices; c) triangularized surface, d) surface with a texture on

Figure 7 shows large deformations of the dog model during an interactive simulation. The combination of the co-rotational FEM-formulation with the coupled mesh technique yields plausible deformational behaviour.



Figure 7: Large plausible deformations of the dog model during interactive simulation

Regarding the objective of “real-time simulation”, the results are, of course, strongly dependent on the hardware used to perform the simulation. The previously described dog model is tested on several available hardware configurations, all of which can be described as “average pc” configurations. The results are summarized in Table 1. As comparison criteria, the ratio between the virtual and real time (‘ratio’ in Table 1; greater than 1 means “faster than real time”), as well as number of frames



		Hardware configuration (processor / graphic card)					
		AMD S140 NVidia 7025		Intel E6750 NVidia 8600 GT		Intel E8500 NVidia 8800 GT	
		Ratio	F/s	Ratio	F/s	Ratio	F/s
Graphics	FE-mesh	3.84	77	4.23	85	5.20	104
	Vertices	1.83	37	2.32	46	3.05	61
	Surface	1.52	30	1.88	38	2.47	49
	Texture	1.11	22	1.08	22	1.63	33

Table 1: Dog model – Efficiency of different hardware configurations

per second ('F/s' in Table 1; vertical synchronization turned off) are chosen. Processors and graphic cards are given as components with the greatest influence on the achieved result, although some other components may play a significant role as well (e.g. motherboard). It should be emphasized that in each case of graphical representation (as given in Figure 6) the simulation is performed so that 5 time-steps, each 0.01 s, are first calculated before the current configuration is depicted on the screen. Although some of the considered processors are dual core processors, the advantage of parallel computing is not used. Additionally, there is still room for optimization in the developed program, as it is only aimed at functionality in the very first step.

2.2.3 Examples – aspect of force feedback

As already noticed, this concept offers a satisfying accuracy when it comes to prediction of structure configuration upon large deformations. The structure may be deformed by predefined displacements or by predefined forces. In the case of predefined displacements the induced internal forces are of importance for specific fields of applications, where force-feedback is required. This is a common requirement for various simulators. However, the presented approach exhibits a weakness regarding the matter, when it is used in its original form. This is a consequence of the fact that behaviour of finite elements in the local c.s. is purely linear, thus neglecting the change in their geometry. The improvement of this aspect requires to observe the change of the element configuration in the local c.s. Hence, the authors of the paper propose an improved novel approach of calculating internal forces for the purpose of force-feedback.

Commonly, force-feedback does not require to evaluate internal elastic forces at all nodes of the FE-mesh, but at a relatively small subset. The elastic forces at that node subset comprise contribution from all the elements that contain at least one of the nodes from the subset. The improvement that the authors propose consists in updating the stiffness matrices of the contributing elements in a specific manner. The idea is to calculate an averaged stiffness between the original and the last determined rotation-free configuration, so that total rotation-free displacements can be used to evaluate the elastic forces. One should notice that this approach differs from the classical tangential approach, where the update of necessary quantities

proceeds incrementally. It is a kind of secant approach that requires only the knowledge of the original and the last determined configuration, without the necessity to know the configurations in-between.

One of the possible ways to perform this is to average the strain-displacement matrix. That would require to store the strain-displacement matrices of each single element for the original configuration, \mathbf{B}_e , given sufficiently available memory, which should not be an issue with modern hardware for models that can be handled at interactive frame rate. Then, the strain-displacement matrix for the last determined rotation-free configuration of an element, ${}^t\mathbf{B}_e^R$, has to be calculated and finally, ${}^0\mathbf{B}_e$ and ${}^t\mathbf{B}_e^R$ are used to average the strain-displacement matrix. A more efficient way would be to determine the mid-configuration between the original and the last determined rotation-free configuration, and then to recalculate the strain-displacement matrix for that configuration, ${}^t\mathbf{B}_{e1/2}$. The stiffness matrix is simply updated:

$${}^t\mathbf{K}_e = \int_{V_e} {}^t\mathbf{B}_e^T \mathbf{H} {}^t\mathbf{B}_{e1/2} dV_e \quad (5)$$

The example of a beam in Figure 8, the length of which is 5 m and cross-section 1×1 m, exposed to predefined free-end displacement is chosen to demonstrate the proposed technique. Again, the model consisting of 25 tetrahedral elements is very simple and it serves only to compare the results of force-elongation diagram for the very same FEM model yielded by ABAQUS, the concept based on rotation of linear stiffness matrices and its modification based on averaged stiffness matrices proposed in this subsection. The example is chosen so that the advantage of the rotation of stiffness matrices is eliminated by large and, therefore, it represents a valid check on the proposed modification. The advantage of the approach based on averaged stiffness compared to the co-rotational formulation is obvious from the diagram in Figure 8.

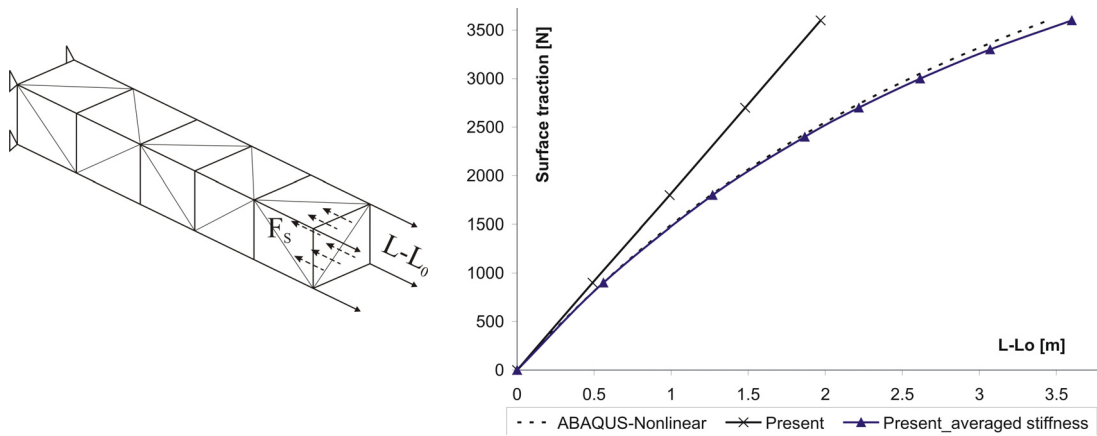


Figure 8: Beam model with surface traction and force-elongation diagram

3 Geometric nonlinearities in simulating flexible bodies in MBS dynamics

Over the last couple of decades, a considerable amount of work has been dedicated to the development of formalisms to simulate flexible bodies in MBS dynamics. The common approach is to describe the deformation of flexible body with respect to a fixed-body reference frame. In that manner, large rigid-body motion is separated from small deformational motion. This provides consideration of nonlinearities resulting from large rigid-body motion, which was actually the original aim of programs for MBS dynamics. Even with this approach the computation of relatively large full FEM models (nodal approach) within the MBS dynamics is a time-consuming and, therefore, rather demanding task.

In order to reduce the computational burden considerably compared to the approach based on the full FEM model, a model reduction is performed. The most common approach is modal approach, which implies that orthogonal mode shapes, calculated in a step prior to simulation, become the degrees of freedom, in terms of which the elastic behaviour of the body is determined. Not only is the number of degrees of freedom in this manner significantly reduced, but the equations for elastic behaviour are also decoupled, i.e. the generalized mass and stiffness matrices are diagonal. The quality of the results obtained with modal approach strongly depends on quality of the mode shapes used in the simulation. The solution used by commercial software package ADAMS is the Component Mode Synthesis (CMS) technique, particularly the Craig-Bampton method. The method requires to partition the flexible body degrees of freedom (DOFs) into boundary DOFs and interior DOFs, the former belonging to the nodes of the FE-model that the user wants to retain in the simulation model mainly for the purpose of defining (kinematic or dynamic) boundary conditions. In the next step, the method requires to determine two sets of modes: 1) *constraint-modes*, which are static shapes obtained by giving each boundary DOF a unit displacement, while all other boundary DOFs are fixed; 2) *fixed-boundary normal modes*, which are obtained by fixing all boundary DOFs and computing an eigensolution. Since the so-obtained Craig-Bampton modes are not an orthogonal set of modes, they are not suitable for direct use in MBS dynamics and are, therefore, orthonormalized prior to simulation.

The modal approach is suitable for small, i.e. linear deformations in the fixed-body reference frame. However, in certain cases (depending on the structure and excitation) the limits of deformations that can be described as 'linear' are exceeded. Considering structures made of engineering materials, the most frequent reason for this is geometrically nonlinear elastic behaviour of structures. Modelling elastic behaviour in such a case is more demanding and requires consideration of geometric nonlinearities. Besides contact problems, geometric nonlinearities can result due to large induced stresses in the structure and also due to relatively large changes in the structure configuration with respect to the body-fixed reference frame. A combination is, of course, also possible. Approaches for the both mentioned causes of geometric nonlinearities are proposed in the following.

3.1 Geometric stiffness matrix

In certain cases of deformational behaviour, induced deformations may be described as ‘small’ compared to dimensions of the structure, although the induced stresses are rather large. Such a case qualifies for extension of linear approach by consideration of stress stiffening effects. This is done through the geometric stiffness matrix.

Geometric stiffness based approach already exists in commercial software package SIMPACK [6]. The software package applies the approach that differentiates between forces, with respect to which the structure is quite flexible (i.e. forces that may cause large deformations) and forces, with respect to which the structure is rather stiff [7]. The latter forces may be quite large, thus inducing significant stresses in the structure, but not large deformations. The large stresses influence the stiffness characteristics of the structure and the influence is accounted for through the geometric stiffness matrix. Since the deformations are small, the stresses are assumed to be linearly dependent on acting forces and the overall stress due to multiple load cases is approximated as a linear superposition of stresses due to each single load case. Those are the same assumptions used in the linear FEM approach.

Geometrically nonlinear FEM calculation can be performed based on total or updated Lagrangian formulation [5]. The difference lies in the choice of reference configuration. A better explanation of the present approach can be provided starting from the total Lagrangian formulation. The tangential stiffness matrix is then given as:

$$\mathbf{K}_T = \mathbf{K}_\theta + \mathbf{K}_u + \mathbf{K}_\sigma, \quad (6)$$

where \mathbf{K}_θ is the linear stiffness matrix of the original configuration, \mathbf{K}_u is the initial displacement matrix that takes into account the displacements between the current and initial structure configuration and, finally, \mathbf{K}_σ is the initial stress (geometric stiffness) matrix, which takes into account the influence of the stress state of the structure on its stiffness.

Adopting the above mentioned assumptions, the tangential stiffness is simplified by neglecting the initial displacement matrix and through a simplified calculation of the geometric stiffness matrix. For each single load case acting on the body the corresponding stress state, σ_θ , is calculated due to unit excitation (force or moment) and, furthermore, the geometric stiffness matrix that corresponds to the stress state caused by unit excitation, $\mathbf{K}_{\sigma\theta}^i$, is calculated. For actual excitation, F_i , the geometric stiffness matrix is simply obtained as:

$$\mathbf{K}_{\sigma i} = F_i \mathbf{K}_{\sigma\theta}^i \quad (7)$$

and finally, the overall stiffness matrix is given as a superposition:

$$\mathbf{K}_\sigma = \sum_{i=1}^n F_i \mathbf{K}_{\sigma\theta}^i \quad (8)$$

Hence, within this approach, the geometric stiffness matrices due to single unit loads are scaled by actual loads and superposed to approximate the actual stiffness matrix. This simplification is justified by previously made assumptions.

The intention of the authors of the paper is to make a step forward with respect to the previously described approach. The idea is to relate the stress states to deformational displacement field rather than to acting forces. The condition for the approach is that the flexible body undergoes relatively small deformations with respect to the fixed-body reference frame. There are certain similarities with the previously presented approach. Namely, for each mode shape the corresponding stress state, σ_0^m , is calculated and, furthermore, the corresponding geometric stiffness matrix, $K_{\sigma 0}^{m_i}$. The current geometric stiffness matrix belonging to a mode is simply obtained by scaling the unit geometric stiffness matrix with modal coefficient, q_i :

$$K_{\sigma i}^m = q_i K_{\sigma 0}^{m_i} \quad (9)$$

and, of course, the overall stiffness matrix is again given as a superposition:

$$K_{\sigma} = \sum_{i=1}^n q_i K_{\sigma 0}^{m_i} \quad (10)$$

One of the steps required for the proposed method is extraction of the geometric stiffness matrices for each mode shape. This is a straightforward task in software packages such as ANSYS or NASTRAN, since they provide this matrix as a standard output. However, in their work the authors used ABAQUS, which provides only the current tangential stiffness matrix, and some inventiveness was required to get the necessary geometric stiffness matrices. The procedure is described below.

For a chosen mode shape, the tangential stiffness matrix for deformed configuration is obtained in the following manner. An analysis is performed in two geometrically nonlinear steps (“nlgeom” on). The first step is static with the excitation given as predefined displacements corresponding to the mode shape. ABAQUS handles predefined displacements by calculating equivalent external forces and by setting large stiffness coefficients (10^{36}) on the main diagonal of the stiffness matrix. The static step is followed by a very short dynamic step ($t = 10^{-10}$ s) with removed predefined displacements, so that the configuration change is absolutely negligible. The only purpose of the dynamic step is to release the boundary conditions, so that the large stiffness coefficients would not occur anymore on the main diagonal of the stiffness matrix. Upon the second step the tangential stiffness matrix is written out as an output.

It is also necessary to obtain the linear stiffness matrix for the deformed shape of the structure corresponding to the mode shape. This is a straightforward task and is done in another analysis, performed as follows. The mode shape displacements are added to the original configuration to get the coordinates of the deformed shape. The so-obtained coordinates are now defined in the input file as an original configuration of the structure, and the tangential stiffness matrix, which is in this case the linear stiffness matrix, is directly written out as an output.

Once both the tangential and linear stiffness matrices for the deformed configuration (deformation according to the mode shape) are known, the geometric stiffness matrix is simply obtained by subtracting the linear stiffness matrix from the tangential stiffness matrix. One may notice that the obtained geometric stiffness matrix is not for the original, but for the deformed configuration. This is the price that has to be paid, since ABAQUS does not offer the geometric stiffness matrix as a standard output. But it should also be noticed that the influence of this aspect can be significantly reduced. A mode shape is determined up to an arbitrary constant and, hence, it can be scaled down by an arbitrary constant. In this way the deformed configuration can be quite close to the original configuration. The scaling factor is further included in the computation to compensate for the mode shape scaling.

Prior to computation of the MBS dynamics, the geometric stiffness matrices for each mode are transformed to modal space in the well-known way [5]. Now, it should be noticed that, according to the proposed method, the current geometric stiffness matrix is a linear function of modal coefficients. The part of internal modal forces due to geometric stiffness can easily be calculated by integration:

$${}^t \vec{f}_{int}^{K\sigma} = \int_0^q \mathbf{K}_{\sigma 0}^m \bar{\bar{q}} \, d\bar{\bar{q}} = \frac{l}{2} \mathbf{K}_{\sigma 0}^m {}^t \bar{\bar{q}}^2 = \frac{l}{2} {}^t \mathbf{K}_{\sigma}^m {}^t \bar{\bar{q}} \quad (11)$$

where subscript t denotes that the quantity is given at time moment t . This fact allows the implementation of the approach in ADAMS.

3.1.1 Example – shell structure with clamped vertices

The above described approach has been implemented in originally developed software as well as in ADAMS.

ADAMS provides a set of user-defined subroutines, which can be used to calculate certain quantities during a simulation. MFOSUB is a type of subroutine that enables the computation of user-defined modal force. The implementation of the proposed technique has been realized through this subroutine. Namely, the part of the internal modal force resulting from the geometric stiffness matrix is calculated by means of Equation (11) and then defined as an external modal force with the opposite sign to that of the internal force.

As for the originally developed software, a simpler approach has been implemented. Over the course of simulation the modal stiffness coefficients are continuously updated by adding the current modal geometric stiffness coefficients to those of the linear modal stiffness matrix.

A rather simple example of a flat shell, the vertices of which are clamped (Figure 9) is considered here to demonstrate the technique. The in-plane dimensions of the shell are 1×0.8 m with thickness of 8 mm. It is made of steel ($E = 2.1 \times 10^{11}$ Pa, $\nu = 0.3$). A force of 7500 N acting transversely upon the shell at its mid-point is chosen so that significant geometrically nonlinear effects are obvious in the behaviour of the structure. In the very beginning of the deformation, bending stiffness determines the structural behaviour. However, as the deformation proceeds, the structure becomes

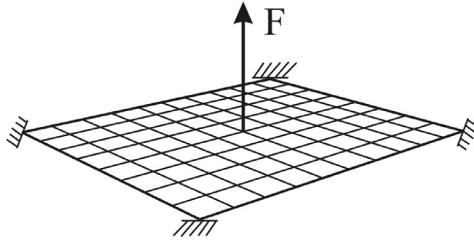


Figure 9: Flat shell with clamped vertices and excitation force

curved and membrane behaviour gains on importance rendering the structure much stiffer. What happens here is an essential change in the way the shell resists the excitation. This is reflected in significant difference between the linear and the geometrically nonlinear result.

The results for the mid-point deflection with different formulations are shown on diagram in Figure 10. The results denoted with ABAQUS are computed with the full FEM model. ADAMS includes nonlinearities as a consequence of single rigid-body rotation. However, the example is chosen so that no rigid-body rotation is present in the structural behaviour. This means that the ADAMS results (denoted with ADAMS in Figure 10) are not affected by this ADAMS feature. The results obtained with the originally developed software are denoted by MODAL. It should be noticed that the linear results from ADAMS and ABAQUS are identical, whereas the linear result from the authors' software differs somewhat. As already elaborated, ADAMS solution is based on orthonormalized Craig-Bampton modes (constraint-modes included) and therefore the excellent agreement with the full FEM result. The authors use only fixed-boundary normal modes in their software. The results denoted with Ksigma are obtained in modal space based formulations (ADAMS and authors' software) with the geometric stiffness matrix included. A good approximation of the full geometrically nonlinear FEM result is observed.

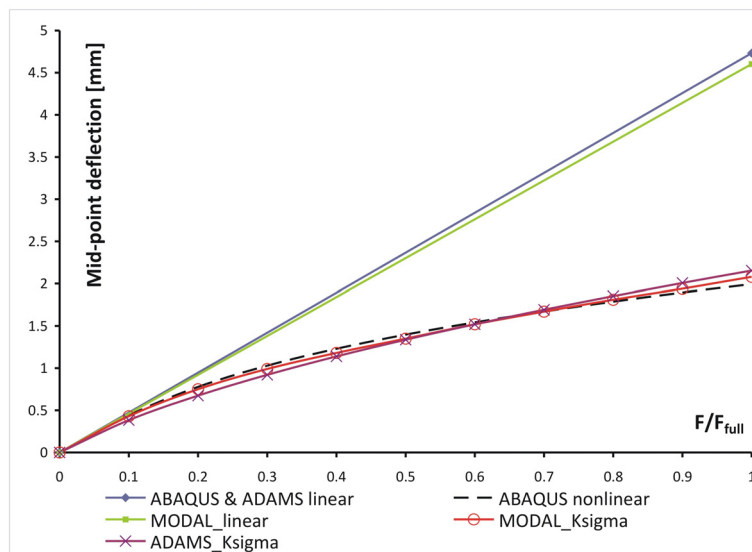


Figure 10: Mid-point deflection of the considered flat shell structure

3.2 Partial rotation of displacements

Geometrically nonlinear behaviour may be caused by relatively large rotation of single domains of the structure with respect to the structure as a whole. Considering moderately large rotations, a modal space based solution, with rigid-body rotation excluded from calculation, would significantly suffer on accuracy of the predicted geometry of deformed structure. Incorporating a single rigid-body rotation into the calculation (as done in MBS software packages), the accuracy of the predicted deformational behaviour might improve in certain cases, but this does not hold for a general case. The authors propose a novel method denoted as partial rotation of displacements.

The idea behind the method can be conveniently described on a very simple structure. Let us observe the clamped beam structure in Figure 11 and consider the deformation corresponding to the first mode shape (Figure 11a). As depicted, the predicted displacement of the beam tip would be such that the tip remains on the line perpendicular to the original configuration. In reality, on the other hand, the tip of the beam would perform a motion similar to the dotted line in Figure 11b. The idea is now presented in Figures 11c and 11d. Firstly, the displacement is calculated as originally yielded by the modal space based solution. In the next step, the average rotation performed by the structure during the motion is calculated (in Figure 11c symbolically presented by angle α). Finally, the amount of rotation determined in the previous step is used to rotate the displacements according to the modal solution, as depicted in Figure 11d. In this case, the approach obviously provides a better approximation of the deformed configuration than the original modal solution.

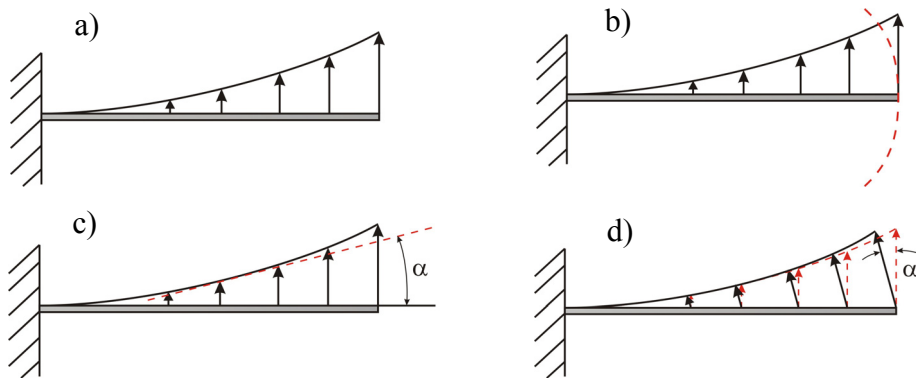


Figure 11: The idea behind the method of partial rotation of displacements

The method has been designed for complex structures, the geometry of which distinguishes several domains that can perform relatively large rigid-body rotations with respect to each other, during deformational behaviour of the whole structure. The idea is to apply the above described approach on single domains. The method is implemented in originally developed software. The user is supposed to define geometrical domains of the structure and to define a set of four representative points for each domain, which are then used to determine the amount of rotation of the domain. A car rear axle is considered below to exemplify the method.

3.2.1 Example – car rear axle

Some typical fields of application of MBS dynamics in car industry are suspension kinematics, handling performance, ride comfort, durability, etc. The increasing number of needed simulations put emphasis onto numerical efficiency, besides the required high degree of accuracy.

Figure 12a depicts the geometry of the considered car rear axle. The full FEM model of the axle has over 300 000 DOFs (courtesy of Volkswagen AG). The deformational behaviour of the axle demands consideration of geometrically nonlinear effects in order to reach the required degree of simulation accuracy. For a single static geometrically nonlinear calculation based on the full FEM model, an ‘average pc configuration’ requires time that may even exceed an hour. On the other hand, the time for modal space based computation is measured in seconds, but the price to be paid is deterioration in accuracy.

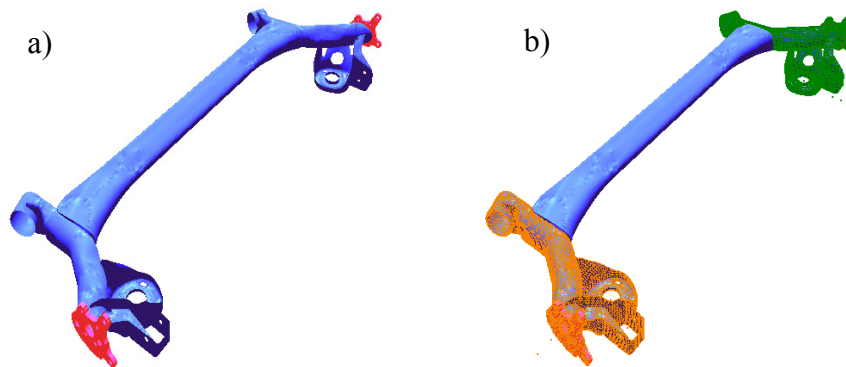


Figure 12: Car rear axle: a) CAD model; b) domains for rotation

The crank arms of the axle are chosen as domains (Figure 12b), for which the displacement rotation is to be performed. This is due to the fact that each arm may perform an average rotation of up to 15° over the course of the axle’s deformation, while deformation of the arms themselves remains rather small. In other words, the arms mainly perform a rigid-body rotation during deformation.

Considering deformational behaviour of a car rear axle, the quantities that are quite often of special interest are vertical wheel displacement (suspension travel) and toe angle. For two specially selected representative load cases, those quantities are calculated with different approaches and represented against each other on diagrams in Figures 13 and 14. Load case 1 is a vertical force of 1 kN acting upon a wheel, while load case 2 is a side force of 7 kN, both of which can be seen in the figures together with the boundary conditions. The reference solution is the geometrically nonlinear one based on the full FEM model. ADAMS solution uses both normal and static modes, and incorporates a single rigid-body rotation. One may notice that this yields a good agreement with the reference solution in the considered cases. The authors’ solution is denoted as Modal_Rotation – it is based on 20 normal modes and the method of partial displacement rotation. Namely, the displacements of the crank arms are regarded separately. The single rigid-body rotation is not included.

This solution also represents a good approximation of the geometrically nonlinear full FEM solution. In certain cases of deformational behaviour, the average rigid-body rotation would be negligible (e.g. the crank arms moving in opposite directions) and the solution based on this technique would suffer on accuracy, whereas the solution based on partial rotation of displacements would still yield a reasonably good approximation of the geometrically nonlinear full FEM solution.

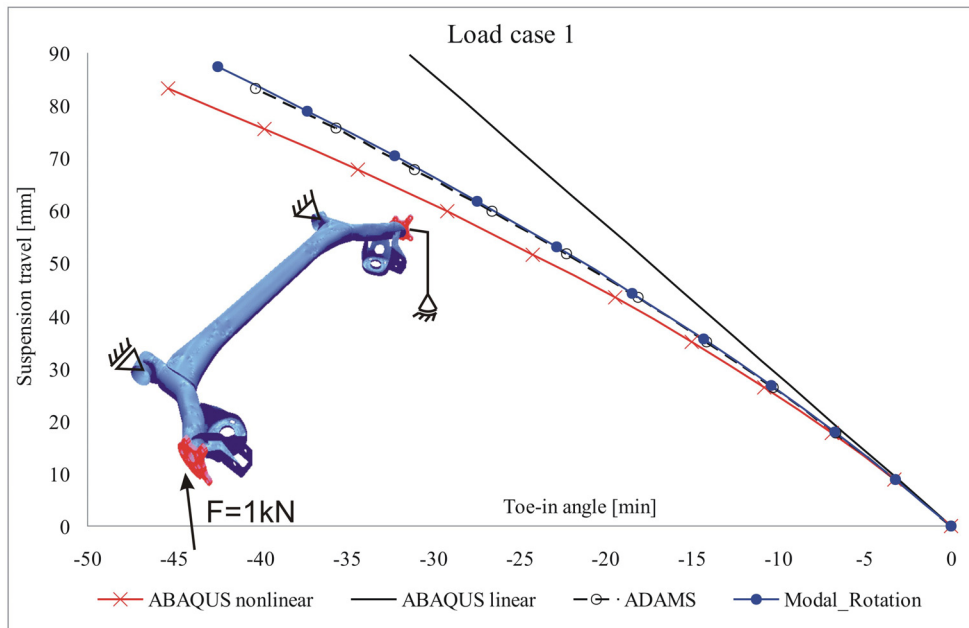


Figure 13: Vertical wheel displacement vs. toe-in angle for load case 1

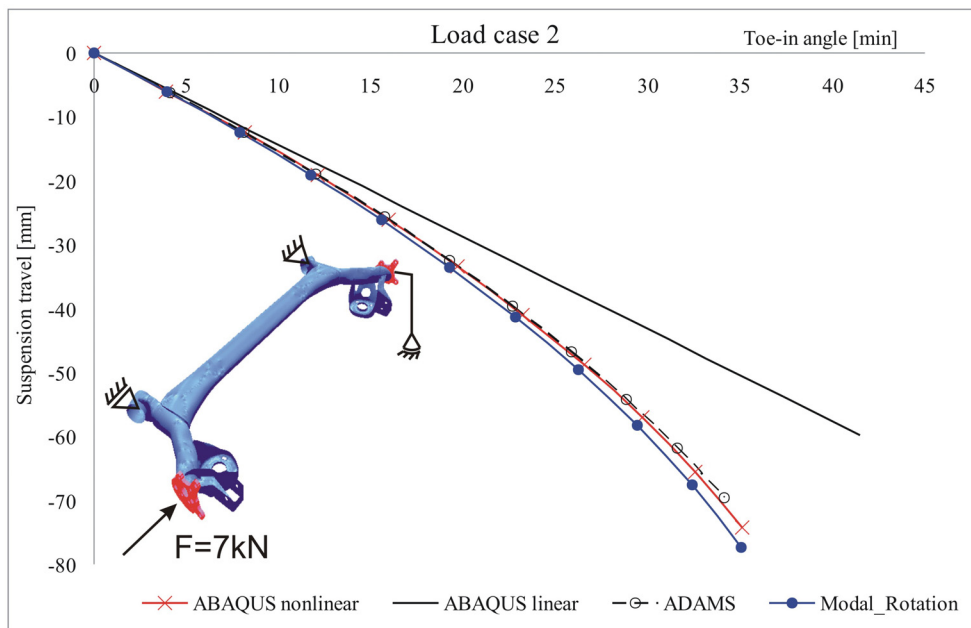


Figure 14: Vertical wheel displacement vs. toe-in angle for load case 2

4 Conclusions

The paper presents FEM approaches for fast computation of geometrically nonlinear deformations. Full FEM as well as modal space based approaches are considered.

The mass-spring systems are rather easy to implement, handle easily large deformations, and are computationally very appealing, but come with serious drawbacks regarding accuracy and ambiguity of model building. The continuum-based FEM approach is much more promising. The presented co-rotational formulation permits to perform a great deal of computation prior to interactive simulation, offers quite satisfying accuracy for typical needs of ‘virtual reality’ systems and the behaviour of models is plausible for quite large deformations. Its drawback regarding the force-feedback can be successfully solved by means of averaged stiffness approach, whereby the computational effort is not significantly increased.

Integration of flexible bodies in MBS dynamics is based on modal space solution. Extension of the approach with the aim of accounting for geometrical nonlinearities is done by the two proposed approaches. One of them considers large stress stiffening effects, whereas the other one accounts for moderately large rotations of single domains of a flexible body. Combined application of both methods is also possible. The choice between the methods is a matter of user’s judgment.

In the future work, it is planned to implement other element types into the proposed co-rotational FEM-formulation, deal with contact problems, plasticity, material tearing, etc. The proposed FE-formulations have a great potential for applications ranging from entertainment industry products, via various types of simulators (e.g. surgery simulators) and up to MBS-dynamics involving flexible bodies.

References

- [1] K. Erlben, J. Sporning, K. Henriksen, H. Dohlmann, “Physics-based animation”, Charles river media, United States, 2005.
- [2] J. Mosegaard, P. Herborg, T.S. Sorensen, “A GPU accelerated spring mass system for surgical simulation”, Studies in health technology and informatics, Vol. 111, pp. 342-348, 2005.
- [3] A. Nealen,, M. Müller, R. Keiser, E. Boxerman, M. Carlson, “Physically based deformable models in computer graphics”, Computer Graphics Forum, Vol. 25(4), pp. 809-836, 2006.
- [4] O. Etmuss, M. Keckeisen, W. Straßer, “A fast finite element solution for cloth modeling”, Proceedings of Pacific Graphics 2003, 2003.
- [5] K. J. Bathe, “Finite element procedures”, Prentice Hall, New Jersey, 1996.
- [6] S. Dietz, O. Wallrapp, S. Wiedemann, „Nodal vs. modal representation in flexible multibody system dynamics“, Proceedings of Multibody Dynamics 2003, IDMEC/IST, Lisbon, 2003.
- [7] R. Schwertassek, O. Wallrapp, “Dynamik flexibler Mehrkörpersysteme”, Vieweg Verlagsgesellschaft, Braunschweig/Wiesbaden, 1999.